A Millennial-Scale Oscillation in Latitudinal Temperature Gradients along the Western North Atlantic during the Mid-Holocene

Bryan N. Shuman[1], Ioana C. Stefanescu[1], Laurie D. Grigg[2], David R. Foster[3], and W. Wyatt Oswald[4]

[1] Department of Geology and Geophysics, University of Wyoming, Laramie, WY.

[2] Department of Earth and Environmental Sciences, Norwich University, Northfield, VT.

[3] Harvard Forest, Harvard University, Petersham, MA.

[4] Marlboro Institute for Liberal Arts and Interdisciplinary Studies, Emerson College, Boston, MA.

Corresponding author: Bryan Shuman (bshuman@uwyo.edu)

Key Points:

- Winter and summer latitudinal temperature gradients changed during the Holocene in eastern North America, including at millennial scales.
- Temperature gradients responded to isolation, ice sheet extent, and millennial-scale dynamics similar to the North Atlantic Oscillation.
- Distributions of major tree taxa were sensitive to the changes, recording different direction changes at different latitudes.

Abstract

Changes in vegetation in North America indicate Holocene shifts in the latitudinal temperature gradient along the western margin of the North Atlantic. The dynamics of tree taxa such as oak (*Quercus*) and hickory (*Carya*) showed opposing directions of change across different latitudes, consistent with changes in temperature gradients. Pollen-inferred temperatures from 34 sites quantify the changes and reconstruct a long-term southward shift of the sharpest temperature gradient in winter and a northward shift in summer. During the mid-Holocene, however, an oscillation in tree distributions interrupted the trends indicating that the steepest portion of the seasonal temperature gradients migrated rapidly northward at 5.8-3.2 ka. The shift produced an unusually late summer thermal maxima at 42-43.5°N where oak abundance peaked both in the early and mid-Holocene. The changes appear consistent with orbital and ice sheet forcing as well as millennial variability in the North Atlantic pressure field during the mid-Holocene.

Plain Language Summary

In the Northern Hemisphere, average temperatures decline with latitude as climates cool toward to the pole. Changes in the temperature pattern have significant consequences for weather systems and the ecosystems affected by them. Summer warmth and winter freezing often determine where tree species can grow. As a result, fossils that show where trees grew in the past offer a unique perspective on past temperatures. In this study, changes in tree distributions over the past 11,700 years revealed that the northward decline in average temperatures near the Atlantic coast of North America fluctuated over time, illustrating a process involved in how climates varied from one millennium to the next. A particularly striking climate change at 5800-3200 years ago caused oak and hickory trees to increase in abundance in mid-latitudes, but decline to the north, steepening the difference between latitude bands. The forest histories demonstrate a strong sensitivity to climate variation, including rapid increases and decreases in tree populations that hint at patterns of a poorly understood timescale of climate variability.

1 Introduction

Temperatures decline steeply with latitude in the northern mid-latitudes, particularly over the eastern areas of the continents. The areas of greatest change are associated with westerly jet streams and create eco-climatic transition zones, such as along the polar front (Bryson, 1966). The location of the front depends upon factors such as topography and land surface conditions (Pielke & Vidale, 1995; Seager et al., 2002), but climate variability such as the North Atlantic Oscillation (NAO) can modify the north-south temperature gradient and the location of its steepest transitions in both summer and winter (Folland et al., 2009; Hurrell et al., 2003). During the Holocene, external forcing also influenced latitudinal temperature gradients with consequences for terrestrial ecosystems (Davis & Brewer, 2009; Routson et al., 2019). Potential variations at centennial to millennial scales have been hard to diagnose (Crucifix et al., 2017; Hernández et al., 2020), but may have been particularly important in the North Atlantic region (O'Brien et al., 1995; Olsen et al., 2012; Orme et al., 2021; Shuman et al., 2019). Reconstructing variations in the latitudinal temperature gradient (LTG), however, could help to evaluate the dynamics driving centennial to millennial climate variations and their ecological consequences.

Holocene tree species' distributions indicate past LTG changes because both growing season warmth and winter freezing temperatures strongly influence plant ranges (Prentice et al., 1991; Woodward, 1987). Centennial-to-millennial temperature changes likely drove shifts in species abundance within previously established tree distributions (Fletcher et al., 2013; Foster et al., 2006; Marsicek et al., 2013). In the North Atlantic region, biogeographic changes can arise from regional LTG responses to the atmospheric pressure difference between the Icelandic low and the North Atlantic sub-tropical high (Hurrell & Deser, 2010). Both pressure systems vary in strength on seasonal (Portis et al., 2001) to orbital time scales (Alder & Hostetler, 2015), likely including centennial to millennial scales (Olsen et al., 2012; Orme et al., 2021). Today, a weak N-S pressure gradient (negative NAO) shifts the steepest portion of the LTG in eastern North America southward as boreal regions warm (Figure 1b), whereas a strong gradient (positive NAO) does the reverse because mid-latitude North America warms (Figure 1c). NAO-like variations at millennial scales could link climate and ecosystem changes in the North Atlantic (Giraudeau et al., 2010; Larsen et al., 2012; Orme et al., 2021), Europe (Fletcher et al., 2013; Vannière et al., 2011), and North America (Shuman, 2022).

To help constrain the synoptic patterns of such climate variations, we used fossil pollen to reconstruct Holocene changes in the LTG over eastern North America. In this region, changes in the LTG during the Pleistocene and early-Holocene depended on the state of the North Atlantic (Fastovich et al., 2020; Levesque et al., 1997; Ruddiman & McIntyre, 1981) and later on the demise of the Laurentide ice sheet and its glacial anti-cyclone (COHMAP, 1988; Shuman et al., 2002). Additional less well diagnosed changes continued into the mid- and late-Holocene. Kirby et al. (2002) used lake oxygen isotopes to infer a rapid southward shift in the polar front in the mid-Holocene. Pollen records show abrupt changes at the same time (Willard et al., 2005). Pollen-inferred summer temperatures declined abruptly at ca. 5 ka across the northern U.S. when they increased 1) to the south from the Great Plains to southern New England (Shuman, 2022; Shuman & Marsicek, 2016) and 2) on average across Europe and North America (Marsicek et al., 2018). Sea-surface temperature reconstructions document different directions of temperature change across latitudes in the western Atlantic at the same time (Lochte et al., 2020; Schmidt et al., 2012).

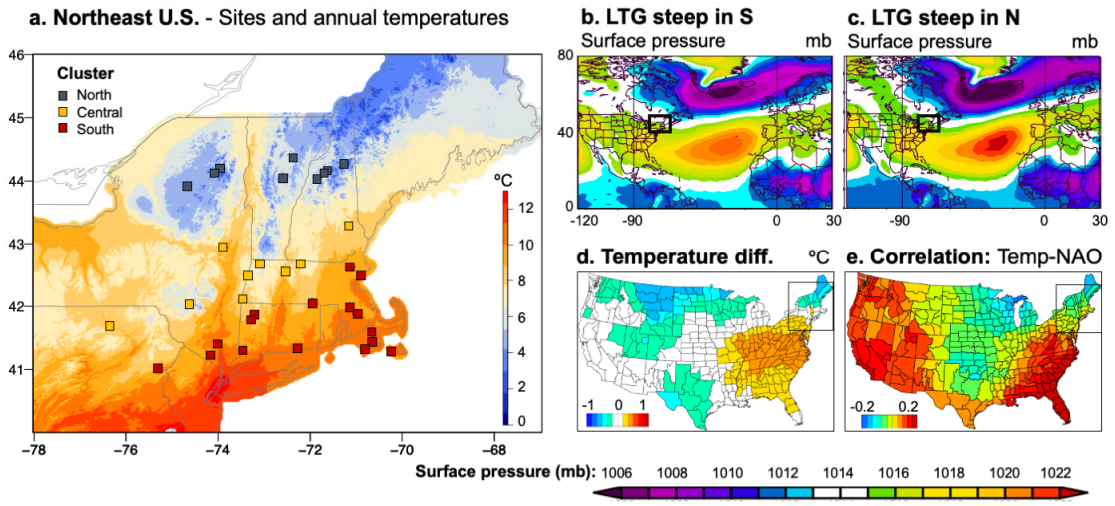

Figure 1. Maps of a) the location of fossil pollen sites, b) years with a steep latitudinal pressure gradient (LTG) in the northern part of the study region (inset box), c) years with a steep LTG in the southern part, d) the mean annual temperature difference between the two sets of years, and e) the annual temperature correlation with the NAO. Modern mean annual temperature across the region (a) are based on 1991-2020 PRISM normals (PRISM 2020); symbols indicate the geographical cluster containing each fossil site. Maps of composite mean surface atmospheric pressures show years when the LTG was steepest b) south of 42.75°N (1960, 1977, 1988, 1999, 2001) and c) north of 42.75°N (1954, 1959, 1968, 1991, 2007). Lower maps represent the d) composite mean temperature differences between each set of years and e) the correlation coefficeient, r, between the NAO and mean annual temperature (T) in each U.S. climate division (Vose et al., 2014).

Here, we reconstruct the Holocene position of the steepest portion of LTG across the northeast U.S. where it is sensitive to the NAO and where modern mean annual temperatures range from <2°C to >12°C (Fig. 1). Fossil pollen records in the study region closely track the climate history (Shuman et al., 2019) and document changes in a strong N-S vegetation gradient (Oswald et al., 2018), which expressed a close association with temperature at the time of European colonization (Cogbill et al., 2002; Thompson et al., 2013). We, therefore, use a dense network of 34 pollen stratigraphies to infer summer and winter temperature history at different latitudes across the region. Latitudinal contrasts in the history of two representative tree genera, oak (*Quercus*) and hickory (*Carya*), underpin the inferred changes in the LTG and highlight the ecological significance of potential millennial-scale climate variability near the North Atlantic.

2 Methods

Detailed fossil pollen records from Connecticut, Massachusetts, New Hampshire, New York, Pennsylvania, and Vermont were obtained from the Neotoma Paleoecological Database (Williams et al., 2018). The records were selected from areas that span the full north-south temperature contrast between 40-45°N latitude. This range of latitudes was possible from 70-

77°W longitude, but not in places to the east, such as Maine. The records span the full Holocene and contain an average of 72 fossil pollen samples (Table S1). Chronologies were updated using intcal20 in bchron (Parnell et al., 2008; Reimer et al., 2020).

We reconstructed mean summer (June-August) and winter (December-February) temperatures using the modern analog technique following the methods of Marsicek et al. (2013), which compared each fossil sample to the best modern analogs from North America east of 95°W using the squared-chord distance metric (Overpeck et al., 1985). The modern pollen samples and their associated temperatures derive from Whitmore et al. (2005). For each fossil pollen sample, the temperatures of the best seven modern analogs were averaged to produce the reconstructed temperature using the R package, *rioja* (Juggins, 2019).

Hierarchical cluster analysis of the summer temperature reconstructions (*hclust* based on Euclidean distances in R)(R Core Development Team, 2022) was used to group the individual records into three ensembles. The clusters were determined from the consistency in their summer temperature reconstructions, which break out by latitude with northern (>43.5°N), central (42-43.5°N), and southern (<42°N) groups of sites, except that eastern coastal sites tended to cluster with the southern group (Fig. 1a). The LTG reconstructions were based on the averages of individual records within each ensemble to reduce reconstruction and chronological uncertainties and remove local ecological effects and noise. Reconstructions were first interpolated to 50-yr intervals to enable averaging on a consistent time scale.

The north-south gradient was measured by assuming that cluster means represent the average temperatures of the three latitudinal bands. The strength of the LTG was calculated as the change in temperature between bands by measuring the central-northern (C-N) and southern-central (S-C) temperature differences; in each case, we subtracted the northern (cooler) cluster mean from the southern (warmer) cluster mean. The two segments were then compared to detect where the LTG was steepest by subtracting the C-N and S-C differences from each other. Positive values in the C-N minus S-C difference indicate a steeper gradient north of 42.75°N, the mid-point of the region, and negative values indicate a steeper gradient to the south.

As context, modern changes in the LTG (shown in Fig. 1) were calculated using the same approach by using annual temperatures from climate division data (Vose et al., 2014); temperature data from Vermont (statewide mean), western Massachusetts (division 1), and Connecticut (statewide mean) represent the northern, central, and southern cluster regions respectively. Composite anomaly maps showing changes in surface pressure and temperatures were generated using the NCEP/NCAR Reanalysis (Kalnay et al., 1996) for the five years when the steepest gradient was furthest north or south based on the C-N (MA-VT) minus S-C (CT-MA) difference, and mapped using tools from the NOAA/ESRL Physical Sciences Laboratory, Boulder, Colorado at https://psl.noaa.gov/.

3 Results

3.1 Reconstructed temperature trends

All of the temperature reconstructions indicate significant early Holocene warming in both summer (Fig. 2) and winter (Fig. 3). At the end of the Younger Dryas at ca. 11.7 ka, summer temperatures increased from 15-16°C to 17.5-18.5°C with all latitudes warming by similar amounts. Summer warming peaked at 18-19°C in the central and northern sites by 8 ka, but southern sites continued to warm, reaching 21°C at 5.5 ka (Fig. 2). In winter, all three

regions continued to warm until 5.5 ka with the greatest rate of warming immediately following the Younger Dryas when all areas increased from <-10°C to >-7°C (Fig. 3). After 10 ka, the southern sites warmed faster in winter than the central and northern sites; by 5.5 ka, southern sites reached near freezing (0°C) even though northern areas only warmed to -5°C (Fig. 3).

After the mid-Holocene, summer temperatures declined in both the northern and southern regions, but not at central sites, which were affected by a significant millennial-scale variation after 5.8 ka (Fig. 2). Initially, northern sites cooled by 0.5°C in both summer (Fig. 2) and winter (Fig. 3). Then, from 4.5-3.2 ka, central sites warmed by 0.5°C in summer (Fig. 2) and 1°C in winter (Fig. 3). After 3.2 ka, northern temperatures remained low in summer, but they warmed again in winter. A second rapid cooling of 0.5°C at 1.5 ka further prevented many northern sites from returning to their previous high summer temperatures.

3.2 Reconstructed gradient changes

The differences between latitudinal clusters indicate that the regional LTG increased over much of the Holocene (Fig. 2d, 3d). Qualitative interpretation of the fossil pollen record also indicates such gradient changes. Oak (*Quercus*), a warmth-adapted genus of broadleaved deciduous trees that flourishes today where summer temperatures exceed 17°C (Williams et al., 2006), increased until ca. 5.5 ka at the southern cluster of sites, but had reached its maximum in the north by 9-8 ka (Fig. 2, green lines). Northern abundance fell to near zero before the 5.5 ka peak was achieved in the south. The opposite patterns of change in oak abundance from 9-5.5 ka, observed over many sites, indicate a widening difference in growing conditions between north and south. The temperature reconstructions based on the full pollen assemblages indicate that the temperature difference increased by 1-1.5°C (Fig. 2d).

A second millennial-scale peak in oak abundance in the central region from 4.6-3.2 ka developed when oak abundance began declining in the south and remained low in the north (Fig. 2, green lines). Consequently, the history of oak indicates a weakening of the southern vegetation and summer temperature gradients from 4.6-3.2 ka as they became steep in the north. The reconstructions indicate that the mid-Holocene anomaly sharply reduced the apparent summer gradient in the south (S-C) by 0.5°C as the northern gradient (C-N) increased by >1°C (Fig. 2d).

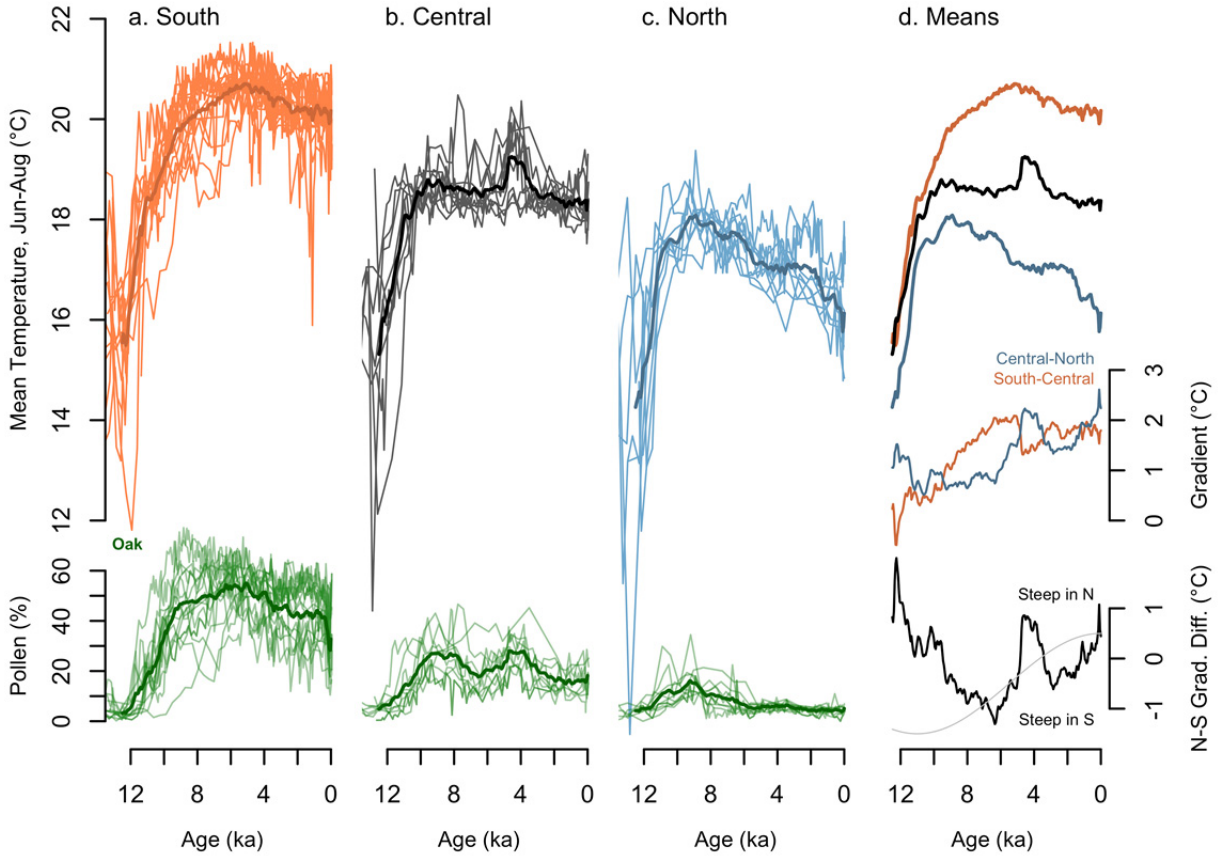

Figure 2. Mean summer (June-August) temperatures and oak (*Quercus*) pollen percentages from a) southern, b) central, and c) northern sites. d) Mean reconstructions for each cluster (bold lines) are shown with their differences and the north minus south difference in gradient steepness ("N-S Grad. Diff." as the black line at bottom right). Positive gradient differences indicate a steeper gradient in the north and negative values indicate steeper in the south. An inverted Northern Hemisphere June insolation curve (Berger, 1978) is normalized to the gradient difference scale for comparison (thin line).

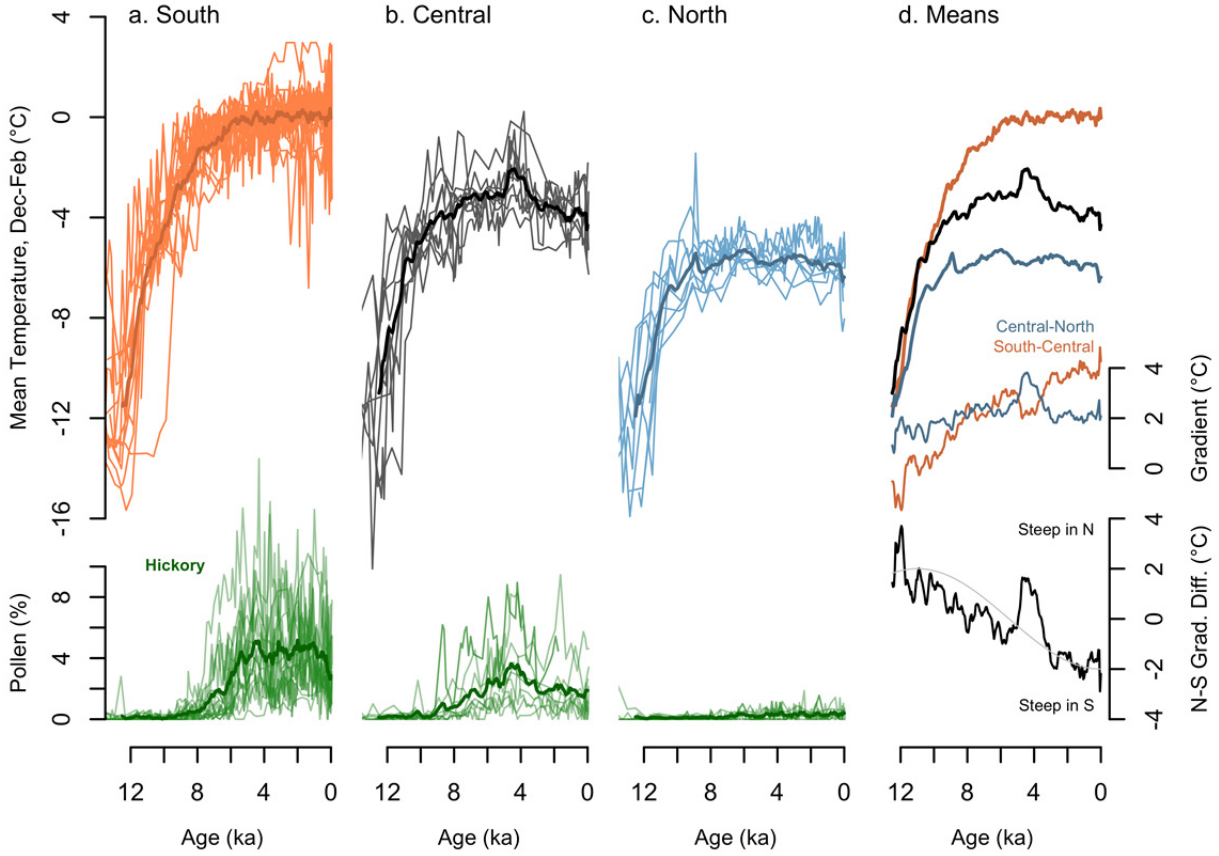

206

207 **Figure 3. As in Figure 2, but for mean winter (December-February) temperatures and**
208 **hickory (Carya) pollen). A Northern Hempisphere January insolation (inverted, gray line)**
209 **is normalized to the N-S gradient difference in d for comparison.**

210 The reconstructed gradients also changed in winter. The patterns appear qualitatively in
211 the Holocene history of hickory (*Carya*), a genus of broadleaved deciduous trees usually
212 restricted in the study area today to areas with mean winter temperatures greater than -4°C
213 (Williams et al., 2006). Unlike oak, hickory is a statistically minor taxon and only became
214 important in the study area after ca. 8 ka (green lines, Fig. 3). Its history parallels the slower
215 long-term increase in temperatures during winter compared to summer. As oak and summer
216 temperatures declined in the late Holocene, hickory retained its earlier abundance suggesting
217 stable winter temperatures.

218 The increase in hickory in the south after 8 ka, but not in the north, marks a widening
219 latitudinal vegetative difference and is reflected by the winter temperature reconstructions
220 generated from the full pollen assemblages. The reconstructions show a persistent C-N
221 difference of ~2°C (thin blue line, Fig. 3d), but a widening S-C difference from near-zero to
222 >4°C (thin red line, Fig. 3d). An exception to this pattern developed from 4.6-3.2 ka when
223 hickory abundance increased in the central region as oak-hickory assemblages typical of the
224 south expanded into central highland sites. Corresponding winter temperature reconstructions
225 indicate a 2°C increase in the C-N gradient and a ~1°C decline in the S-C gradient (Fig. 3d).

3.3 Changing latitude of steepest gradients

The difference in the steepness of the two summer temperature gradients (the C-N minus S-C gradient difference, bottom panel, Fig. 2d) indicates

- a southward shift in the steepest part of the gradient before 6 ka as the C-N difference remained stable but the S-C difference increased;
- a millennial oscillation from 4.6-3.2 ka when the northern (C-N) gradient became steeper than the southern (S-C) gradient by up to 0.8°C; and then
- a northward shift in the steepest portion of the gradient (a positive gradient difference, Fig. 2d) after 3.2 ka.

In winter, because the northern (C-N) gradient remained near 2°C and the southern (S-C) gradient increased from 0°C to >4°C, the gradient was initially steepest in the north but shifted to the south, even following the northward oscillation from 4.6-3.2 ka when C-N was steeper than S-C by up to 1.6°C (Fig. 3d).

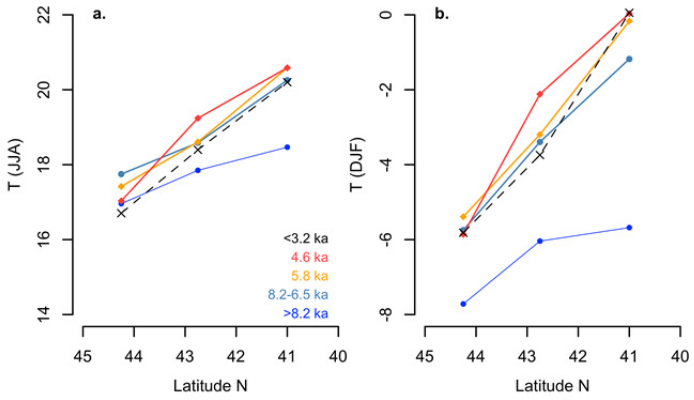

Figure 4. Reconstructed latitudinal temperatures for a) summer (July-August, JJA) and b) winter (December-February, DJF) on average at >8.2 ka (dark blue), from 8.2-6.5 ka (light blue), and since 3.2 ka (black) for comparison with those at 5.8 ka (orange) and 4.6 ka (red).

4 Discussion

4.1 Interpreting the vegetation changes

A modern association between ecotones and the steepest fronts in the LTG has long been recognized (Bryson, 1966; Pielke & Vidale, 1995). At the time of European colonization of the northeastern U.S., the LTG determined a sharp contrast between northern mixed forests and oak-hickory forests to the south (Cogbill et al., 2002). Oak and hickory had similar distributions in the study region at the time, but their different seasonal temperature sensitivities are underscored by strikingly different historic distributions in the central U.S. where continental summer and winter temperature patterns differ, limiting hickory's northern extent (Paciorek et al., 2016, 2021; Prentice et al., 1991). The Holocene abundances of these and other regional tree taxa have similarly been linked to temperature changes since the earliest palynological studies (Deevey, 1939). Indeed, direct comparisons between fossil pollen and independent paleoclimate data from

the northeast U.S. reveal a tight coupling with no significant lags at >100 yr time scales (Shuman et al., 2019).

The reconstructed shifts in the LTG, therefore, provide a plausible climatic explanation for spatial differences in the histories of warm-tolerant oak and hickory populations among others. A weak north-south gradient in summer before ca. 6.5 ka (light blue line, Figure 4a) helps to explain the early peak in oak abundance at northern sites (green lines, Figure 2c); the polar front was likely furthest north at the time, extending similar summer temperatures across the region and enabling oak to spread widely. If the summer LTG then steepened by 5.8 ka (Figure 2d), oak could have readily declined where sites began cooling in the north (Figure 2c) while expanding into newly warmed central areas (Figure 2b). Tree population increases south of a non-advancing range limit are not uncommon (Lloyd, 2005), especially if the LTG were to steepen rather than to produce uniform temperatures increases or declines regionwide (Figure 4).

Other alternative interpretations do not explain the spatial complexity of the observed vegetation changes. For example, dispersal lags would not have been important because oak and hickory were established across the study area early in the Holocene. Ecological and statistical percentage effects of a range-wide decline of hemlock (*Tsuga*) populations at ca. 5.5-5.0 ka also should have applied across the entire region and do not explain why oak would have increased only in the central region while declining in others (Foster et al., 2006). Climatic influences rather than short-lived successional dynamics also clarify why oak increased at 4.6-3.2 ka after shade-tolerant, late-successional taxa like beech (*Fagus*) increased at the same sites from 5.0-4.6 ka (Oswald et al., 2007, 2018; Whitehead & Crisman, 1978). Additionally, the modern analog technique used here simultaneously produces independently-validated precipitation reconstructions (Shuman et al., 2019) and accounts for the interacting role of moisture on the pollen assemblages when reconstructing temperatures (Williams and Shuman 2008).

4.2 Climate dynamics involved

Different directions of insolation forcing over the Holocene explain much of the northward steepening of the summer LTG (Fig. 2d) and southward steepening of the winter LTG (Fig. 3d). Early-to-mid Holocene insolation anomalies acted to weaken the summer LTG (Fig. 4a) by preferentially heating northern continental areas, especially compared to coastal areas in the south. The winter LTG also strengthened since the early Holocene (Fig. 4b) because insolation anomalies cooled low latitudes more than high latitudes, which receive little winter insolation even today (Berger, 1978). A southward shift in the summer LTG during the early-Holocene, however, represents a departure from the insolation trend (black line, bottom, Fig. 2d). Much of the change, prior to ca. 8 ka, appears consistent with a weak north-south pressure gradient when the Laurentide ice sheet remained influential. The summer anomaly may conflict with expectations of an insolation-driven strengthening of the pressure gradient (Alder & Hostetler, 2015), but could indicate that a thermodynamic response to the ice albedo anomaly likely generated the pattern (Morrill et al., 2018) rather than the year-round effect of the ice as a mechanical barrier to the flow of the jet stream (COHMAP, 1988).

The most significant departure from the insolation and ice sheet effects arises as a pronounced northward shift in the steepest portion of the gradient after 5.8 ka. Despite the opposing directions of long-term change between seasons in the late-Holocene, the summer and winter expression of the mid-Holocene oscillation were similar. The similar patterns may relate to challenges separately reconstructing climate variables that are correlated today, but the large

differences in the summer and winter LTG reconstructions overall indicate that the anomaly may well apply to both seasons. Both anomalies began as temperatures fell in the north at 5.8 ka (bold blue lines, Fig. 2d, 3d) and were then amplified when temperatures in the central region increased sharply at 4.8-3.7 ka (bold black lines, Fig. 2d, 3d). The initial cooling at northern sites agrees with isotopic evidence from northern sites (Kirby et al., 2002; Shuman & Marsicek, 2016). Such a steepening and northward shift in the LTG develops during positive summer NAO phases today (Folland et al., 2009). Temperature anomalies today develop in central areas, such as western Massachusetts, as an extension of warming in the mid-Atlantic region, but are surrounded by little change in the southern part of our study area (Fig. 1d).

Low sea-surface temperatures (SSTs) from 4.5-3.5 ka on the Labrador Shelf (Lochte et al., 2020) and coincident high SSTs in the Florida Strait from 4.7-3.3 ka (Schmidt et al., 2012) agree with the anti-phased SST anomalies along the North American margin expected from patterns associated with a strong Atlantic pressure gradient (Fig. S1). However, a correlated NAO reconstruction from lake sediments in Greenland records the opposite sign phase (Olsen et al., 2012), which raises questions about the specific circulation changes involved and whether they have direct analogs to the NAO at monthly to annual scales. Regardless of the relationship to NAO phases or not, the oscillation coincides with prominent features in other North Atlantic records, which indicate millennial anomalies in deep water flow, wind speeds, and atmospheric circulation (Giraudeau et al., 2010; Jackson et al., 2005; O'Brien et al., 1995) when evidence of unusual climates extended from submerged tree stumps in Lake Tahoe, California (Benson et al., 2002) and paleosol development in Nebraska's Sand Hills (Miao et al., 2007) to millennial temperature and isotopic anomalies in Africa (Berke et al., 2012; Thompson et al., 2002).

The millennial-scale shifts in the LTG and Atlantic pressure gradient may relate to intrinsic atmospheric variability on interannual time scales (Folland et al., 2009; Hurrell et al., 2003), particularly given the potential involvement of ocean-atmosphere or sea-ice interactions to sustain variations over centuries to millennia during the mid-Holocene (Orme et al., 2021; Rigor et al., 2002; Thornalley et al., 2009). Alternatively, volcanic and solar variability may have been influential factors (Fletcher et al., 2013; Kobashi et al., 2017), but no clear linear correlation with external forcing is evident, potentially as expected (Renssen et al., 2006).

5 Conclusions

The Holocene temperature history of eastern North America includes changes in the steepness of the north-south temperature gradient, which generally responded in different directions to summer and winter insolation anomalies. Well-described Holocene forcing, however, does not explain an apparent millennial-scale latitudinal shift in the slope and position of the temperature front, which expanded oak-hickory forests into mid-latitudes as they declined to the north from 5.8-3.2 ka. Understanding the NAO-like change may help explain other mid-Holocene abrupt change events and dynamics.

Acknowledgments

This work was supported by NSF funding to BNS (DEB-1856047) and to the Harvard Forest Long-Term Ecological Research Program (LTER-1832210).

Open Research

The analyses here depend upon fossil pollen data, which can be retrived from the Neotoma Paleoecology Database using the site names listed in Table S1 in the 'neotoma' package version 1.7.4 in R 4.0.0 (Goring et al., 2019; R Core Development Team, 2022). Chronologies were updated in R using the 'bchron' package version 4.7.4 (Parnell et al., 2008) and temperature reconstructions were generated using the 'rioja' package version 0.9-21 (Juggins, 2019). The reconstructions and median ages are available as a supplement to this manuscript and will be submitted to the NOAA NCEI Paleoclimate archive upon acceptance for publication.

References

Alder, J. R., & Hostetler, S. W. (2015). Global climate simulations at 3000-year intervals for the last 21 000 years with the GENMOM coupled atmosphere–ocean model. *Climate of the Past*, *11*(3), 449–471.

Benson, L., Kashgarian, M., Rye, R., Lund, S., Paillet, F., Smoot, J., et al. (2002). Holocene multidecadal and multicentennial droughts affecting Northern California and Nevada. *Quaternary Science Reviews*, *21*(4–6), 659–682.

Berger, A. (1978). Long-term variations of caloric insolation resulting from the earth's orbital elements. *Quaternary Research*, *9*(2), 139–167.

Berke, M. A., Johnson, T. C., Werne, J. P., Schouten, S., & Sinninghe Damsté, J. S. (2012). A mid-Holocene thermal maximum at the end of the African Humid Period. *Earth and Planetary Science Letters*, *351–352*, 95–104. https://doi.org/10.1016/j.epsl.2012.07.008

Bryson, R. A. (1966). Air masses, streamlines, and the boreal forest. *Geological Society of America Bulletin*, *8*, 228.

Cogbill, C. V., Burk, J., & Motzkin, G. (2002). The forests of presettlement New England, USA: spatial and compositional patterns based on town proprietor surveys. *Journal of Biogeography*, *29*(10–11), 1279–1304. https://doi.org/10.1046/j.1365-2699.2002.00757.x

COHMAP Members (1988). Climate changes of the last 18,000 years: observations and model simulations. *Science*, *241*, 1043–1052.

Crucifix, M., de Vernal, A., Franzke, C., & von Gunten, L. (2017). Centennial to Millennial Climate Variability, 131–166. https://doi.org/10.22498/pages.25.3

Davis, B. A., & Brewer, S. (2009). Orbital forcing and role of the latitudinal insolation/temperature gradient. *Climate Dynamics*, *32*(2–3), 143–165. http://dx.doi.org/10.1007/s00382-008-0480-9

Deevey, E. S. (1939). Studies on Connecticut lake sediments. I. A Postglacial Climatic Chronology for Southern New England. *American Journal of Science*, *237*, 691–724.

Fastovich, D., Russell, J. M., Jackson, S. T., Krause, T. R., Marcott, S. A., & Williams, J. W. (2020). Spatial Fingerprint of Younger Dryas Cooling and Warming in Eastern North America. *Geophysical Research Letters*, *47*(22), e2020GL090031. https://doi.org/10.1029/2020GL090031

Fletcher, W. J., Debret, M., & Goñi, M. F. S. (2013). Mid-Holocene emergence of a low-frequency millennial oscillation in western Mediterranean climate: Implications for past dynamics of the North Atlantic atmospheric westerlies. *The Holocene*, *23*(2), 153–166. https://doi.org/10.1177/0959683612460783

Folland, C. K., Knight, J., Linderholm, H. W., Fereday, D., Ineson, S., & Hurrell, J. W. (2009). The Summer North Atlantic Oscillation: Past, Present, and Future. *Journal of Climate*, *22*(5), 1082–1103. https://doi.org/10.1175/2008JCLI2459.1

Foster, D. R., Oswald, W. W., Faison, E. K., Doughty, E. D., & Hansen, B. C. S. (2006). A climatic driver for abrupt mid-Holocene vegetation dynamics and the hemlock decline in New England. *Ecology*, *87*(12), 2959–2966.

Giraudeau, J., Grelaud, M., Solignac, S., Andrews, J. T., Moros, M., & Jansen, E. (2010). Millennial-scale variability in Atlantic water advection to the Nordic Seas derived from Holocene coccolith concentration records. *Quaternary Science Reviews*, *29*(9), 1276–1287. https://doi.org/10.1016/j.quascirev.2010.02.014

Goring, S. J., Simpson, G. L., Marsicek, J. P., Ram, K., & Sosalla, L. (2019). neotoma: Programmatic R interface to the Neotoma Paleoecological Database. R, rOpenSci. Retrieved from https://github.com/ropensci/neotoma

Hernández, A., Martin-Puertas, C., Moffa-Sánchez, P., Moreno-Chamarro, E., Ortega, P., Blockley, S., et al. (2020). Modes of climate variability: Synthesis and review of proxy-based reconstructions through the Holocene. *Earth-Science Reviews*, *209*, 103286. https://doi.org/10.1016/j.earscirev.2020.103286

Hurrell, J. W., & Deser, C. (2010). North Atlantic climate variability: The role of the North Atlantic Oscillation. *Journal of Marine Systems*, *79*(3), 231–244. https://doi.org/10.1016/j.jmarsys.2009.11.002

Hurrell, J. W., Kushnir, Y., Ottersen, G., & Visbeck, M. (2003). *The North Atlantic Oscillation*. *Geophys. Monogr. Ser.* (Vol. 134). https://doi.org/10.1029/134GM01

Jackson, M. G., Oskarsson, N., Trønnes, R. G., McManus, J. F., Oppo, D. W., Grönvold, K., et al. (2005). Holocene loess deposition in Iceland: Evidence for millennial-scale atmosphere-ocean coupling in the North Atlantic. *Geology*, *33*(6), 509–512. https://doi.org/10.1130/G21489.1

Juggins, S. (2019). rioja: Analysis of Quaternary Science Data (Version 0.9-21). Retrieved from https://CRAN.R-project.org/package=rioja

Kalnay, E., Kanamitsu, M., Kistler, R., Collins, W., Deaven, D., Gandin, L., et al. (1996). The NCEP/NCAR 40-Year Reanalysis Project. *Bulletin of the American Meteorological Society*, *77*(3), 437–472. https://doi.org/10.1175/1520-0477(1996)077<0437:TNYRP>2.0.CO;2

Kirby, M. E., Mullins, H. T., Patterson, W. P., & Burnett, A. W. (2002). Late glacial-Holocene atmospheric circulation and precipitation in the northeast United States inferred from modern calibrated stable oxygen and carbon isotopes. *Geological Society of America Bulletin*, *114*(10), 1326–1340. https://doi.org/10.1130/0016-7606(2002)114<1326:lghaca>2.0.co;2

Kobashi, T., Menviel, L., Jeltsch-Thömmes, A., Vinther, B. M., Box, J. E., Muscheler, R., et al. (2017). Volcanic influence on centennial to millennial Holocene Greenland temperature change. *Scientific Reports*, *7*(1), 1441. https://doi.org/10.1038/s41598-017-01451-7

Larsen, D. J., Miller, G. H., Geirsdóttir, Á., & Ólafsdóttir, S. (2012). Non-linear Holocene climate evolution in the North Atlantic: a high-resolution, multi-proxy record of glacier activity and environmental change from Hvítárvatn, central Iceland. *Quaternary Science Reviews*, *39*, 14–25. https://doi.org/10.1016/j.quascirev.2012.02.006

Levesque, A. J., Cwynar, L. C., & Walker, I. R. (1997). Exceptionally steep north-south gradients in lake temperatures during the last deglaciation. *Nature*, *385*(6615), 423–426.

418 Lloyd, A. H. (2005). Ecological histories from Alaskan tree lines provide insight into future change. *Ecology*, *86*(7),
419 1687–1695.
420 Lochte, A. A., Schneider, R., Kienast, M., Repschläger, J., Blanz, T., Garbe-Schönberg, D., & Andersen, N. (2020).
421 Surface and subsurface Labrador Shelf water mass conditions during the last 6000 years. *Climate of the*
422 *Past*, *16*(4), 1127–1143. https://doi.org/10.5194/cp-16-1127-2020
423 Marsicek, J. P., Shuman, B., Brewer, S., Foster, D. R., & Oswald, W. W. (2013). Moisture and temperature changes
424 associated with the mid-Holocene Tsuga decline in the northeastern United States. *Quaternary Science*
425 *Reviews*, *80*(3), 333–342. https://doi.org/10.1016/j.quascirev.2013.09.001
426 Marsicek, J. P., Shuman, B. N., Bartlein, P. J., Shafer, S. L., & Brewer, S. (2018). Reconciling divergent trends and
427 millennial variations in Holocene temperatures. *Nature*, *554*(7690), 92–96.
428 https://doi.org/10.1038/nature25464
429 Miao, X., Mason, J. A., Johnson, W. C., & Wang, H. (2007). High-resolution proxy record of Holocene climate
430 from a loess section in Southwestern Nebraska, USA. *Palaeogeography, Palaeoclimatology,*
431 *Palaeoecology*, *245*(3–4), 368–381. https://doi.org/10.1016/j.palaeo.2006.09.004
432 Morrill, C., Lowry, D. P., & Hoell, A. (2018). Thermodynamic and Dynamic Causes of Pluvial Conditions During
433 the Last Glacial Maximum in Western North America. *Geophysical Research Letters*, *45*(1), 335–345.
434 https://doi.org/10.1002/2017GL075807
435 O'Brien, S. R., Mayewski, P., Meeker, L. D., Twickler, M. S., & Whitlow, S. I. (1995). Complexity of Holocene
436 climate as reconstructed from a Greenland ice core. *Science*, *270*, 1962.
437 Olsen, J., Anderson, N. J., & Knudsen, M. F. (2012). Variability of the North Atlantic Oscillation over the past
438 5,200 years. *Nature Geoscience*, *5*(11), 808–812. https://doi.org/10.1038/ngeo1589
439 Orme, L. C., Miettinen, A., Seidenkrantz, M.-S., Tuominen, K., Pearce, C., Divine, D. V., et al. (2021). Mid to late-
440 Holocene sea-surface temperature variability off north-eastern Newfoundland and its linkage to the North
441 Atlantic Oscillation. *The Holocene*, *31*(1), 3–15. https://doi.org/10.1177/0959683620961488
442 Oswald, W. W., Faison, E. K., Foster, D. R., Doughty, E. D., Hall, B. R., & Hansen, B. C. S. (2007). Post-glacial
443 changes in spatial patterns of vegetation across southern New England. *Journal of Biogeography*, *34*(5),
444 900–913. https://doi.org/10.1111/j.1365-2699.2006.01650.x

Oswald, W. W., Foster, D. R., Shuman, B. N., Doughty, E. D., Faison, E. K., Hall, B. R., et al. (2018). Subregional variability in the response of New England vegetation to postglacial climate change. *Journal of Biogeography*, *45*(10), 2375–2388. https://doi.org/10.1111/jbi.13407

Overpeck, J. T., Webb III, T., & Prentice, I. C. (1985). Quantitative interpretation of fossil pollen spectra: dissimilarity coefficients and the method of modern analogs. *Quaternary Research*, *23*, 87–108.

Paciorek, C. J., Goring, S. J., Thurman, A. L., Cogbill, C. V., Williams, J. W., Mladenoff, D. J., et al. (2016). Statistically-estimated tree composition for the northeastern United States at Euro-American settlement. *PloS One*, *11*(2), e0150087.

Paciorek, C. J., Cogbill, C. V., Peters, J. A., Williams, J. W., Mladenoff, D. J., Dawson, A., & McLachlan, J. S. (2021). The forests of the midwestern United States at Euro-American settlement: Spatial and physical structure based on contemporaneous survey data. *PLOS ONE*, *16*(2), e0246473. https://doi.org/10.1371/journal.pone.0246473

Parnell, A. C., Haslett, J., Allen, J. R. M., Buck, C. E., & Huntley, B. (2008). A flexible approach to assessing synchroneity of past events using Bayesian reconstructions of sedimentation history. *Quaternary Science Reviews*, *27*(19â€“20), 1872–1885. https://doi.org/10.1016/j.quascirev.2008.07.009

Pielke, R. A., & Vidale, P. L. (1995). The boreal forest and the polar front. *Journal of Geophysical Research: Atmospheres*, *100*(D12), 25755–25758. https://doi.org/10.1029/95JD02418

Portis, D. H., Walsh, J. E., El Hamly, M., & Lamb, P. J. (2001). Seasonality of the North Atlantic Oscillation. *Journal of Climate*, *14*(9), 2069–2078.

Prentice, I. C., Bartlein, P. J., & Webb III, T. (1991). Vegetation and climate changes in eastern North America since the last glacial maximum: A response to continuous climatic forcing. *Ecology*, *72*, 2038–2056.

R Core Development Team. (2022). *R: A language and environment for statistical computing.* R Foundation for Statistical Computing, Vienna, Austria. Retrieved from http://www.R-project.org

Reimer, P. J., Austin, W. E. N., Bard, E., Bayliss, A., Blackwell, P. G., Ramsey, C. B., et al. (2020). The IntCal20 Northern Hemisphere Radiocarbon Age Calibration Curve (0–55 cal kBP). *Radiocarbon*, *62*(4), 725–757. https://doi.org/10.1017/RDC.2020.41

Renssen, H., Goosse, H., & Muscheler, R. (2006). Coupled climate model simulation of Holocene cooling events: oceanic feedback amplifies solar forcing. *Climate of the Past*, *2*, 79–90.

Rigor, I. G., Wallace, J. M., & Colony, R. L. (2002). Response of Sea Ice to the Arctic Oscillation. *Journal of Climate*, *15*(18), 2648–2663. https://doi.org/10.1175/1520-0442(2002)015<2648:ROSITT>2.0.CO;2

Routson, C. C., McKay, N. P., Kaufman, D. S., Erb, M. P., Goosse, H., Shuman, B. N., et al. (2019). Mid-latitude net precipitation decreased with Arctic warming during the Holocene. *Nature*, *568*(7750), 83–87. https://doi.org/10.1038/s41586-019-1060-3

Ruddiman, W. F., & McIntyre, A. (1981). The North Atlantic Ocean during the last deglaciation. *Palaeogeography, Palaeoclimatology, Palaeoecology*, *35*, 145–214.

Schmidt, M. W., Weinlein, W. A., Marcantonio, F., & Lynch-Stieglitz, J. (2012). Solar forcing of Florida Straits surface salinity during the early Holocene. *Paleoceanography*, *27*(3). https://doi.org/10.1029/2012PA002284

Seager, R., Battisti, D. S., Yin, J., Gordon, N., Naik, N., Clement, A. C., & Cane, M. A. (2002). Is the Gulf Stream responsible for Europe's mild winters? *Quarterly Journal of the Royal Meteorological Society*, *128*(586), 2563–2586. https://doi.org/10.1256/qj.01.128

Shuman, B. N. (2022). Centennial-to-Millennial Holocene Temperature and Hydroclimate Variation in the Northern Mid-Latitudes. *Climates of the Past Discussion*. https://doi.org/10.5194/cp-2022-89

Shuman, B. N., & Marsicek, J. P. (2016). The Structure of Holocene Climate Change in Mid-Latitude North America. *Quaternary Science Reviews*, *141*, 38–51.

Shuman, B. N., Bartlein, P., Logar, N., Newby, P., & Webb, T. (2002). Parallel climate and vegetation responses to the early-Holocene collapse of the Laurentide Ice Sheet. *Quaternary Science Reviews*, *21*, 1793–1805.

Shuman, B. N., Marsicek, J., Oswald, W. W., & Foster, D. R. (2019). Predictable hydrological and ecological responses to Holocene North Atlantic variability. *Proceedings of the National Academy of Sciences*, *116*(13), 5985–5990. https://doi.org/10.1073/pnas.1814307116

Thompson, J. R., Carpenter, D. N., Cogbill, C. V., & Foster, D. R. (2013). Four Centuries of Change in Northeastern United States Forests. *PLOS ONE*, *8*(9), e72540. https://doi.org/10.1371/journal.pone.0072540

Thompson, L. G., Mosley-Thompson, E., Davis, M. E., Henderson, K. A., Brecher, H. H., Zagorodnov, V. S., et al. (2002). Kilimanjaro Ice Core Records: Evidence of Holocene Climate Change in Tropical Africa. *Science*, *298*(5593), 589–593. https://doi.org/10.1126/science.1073198

500 Thornalley, D. J. R., Elderfield, H., & McCave, I. N. (2009). Holocene oscillations in temperature and salinity of the
501 surface subpolar North Atlantic. *Nature*, *457*(7230), 711–714.
502 Vannière, B., Power, M. J., Roberts, N., Tinner, W., Carrión, J., Magny, M., et al. (2011). Circum-Mediterranean
503 fire activity and climate changes during the mid-Holocene environmental transition (8500-2500 cal. BP).
504 *The Holocene*, *21*(1), 53–73. http://dx.doi.org.libproxy.uwyo.edu/10.1177/0959683610384164
505 Whitehead, D. R., & Crisman, T. (1978). Paleolimnological studies of small New England (U.S.A.) ponds. I: Late
506 glacial and postglacial trophic oscillations. *Polskie Archiwum Hydrobiologii*, *25*, 471–481.
507 Whitmore, J., Gajewski, K., Sawada, M., Williams, J., Shuman, B., Bartlein, P. J., et al. (2005). An updated modern
508 pollen-climate-vegetation dataset for North America. *Quaternary Science Reviews*, *24*, 1828–1848.
509 Willard, D. A., Bernhardt, C. E., Korejwo, D. A., & Meyers, S. R. (2005). Impact of millennial-scale Holocene
510 climate variability on eastern North American terrestrial ecosystems: pollen-based climatic reconstruction.
511 *Global and Planetary Change*, *47*(1), 17–35. https://doi.org/10.1016/j.gloplacha.2004.11.017
512 Williams, J. W., Shuman, B. N., Bartlein, P. J., Whitmore, J., Gajewski, K., Sawada, M., et al. (2006). An Atlas of
513 Pollen-Vegetation-Climate Relationships for the United States and Canada. *American Association of*
514 *Stratigraphic Palynologists Foundation, Dallas, TX*.
515 Williams, J. W., Grimm, E. C., Blois, J. L., Charles, D. F., Davis, E. B., Goring, S. J., et al. (2018). The Neotoma
516 Paleoecology Database, a multiproxy, international, community-curated data resource. *Quaternary*
517 *Research*, *89*(1), 156–177. https://doi.org/10.1017/qua.2017.105
518 Woodward, F. I. (1987). *Climate and Plant Distribution*. (R. S. K. Barnes, H. J. B. Birks, E. F. Connor, J. L. Harper,
519 & R. T. Paine, Eds.). Cambridge: Cambridge University Press.
520 Vose, R.S., Applequist, S., Durre, I., Menne, M.J., Williams, C.N., Fenimore, C., et al. (2014). Improved Historical
521 Temperature and Precipitation Time Series For U.S. Climate Divisions. *Journal of Applied Meteorology*
522 *and Climatology*. http://dx.doi.org/10.1175/JAMC-D-13-0248.1

523
524